Coupled Systems Mechanics, *Vol. 11, No. 6 (2022) 557-586*
https://doi.org/10.12989/csm.2022.11.6.557

The effectiveness of position of coupled beam with respect to the floor level

Yasser Abdal Shafey Gamal[1] and Lamiaa K. Idriss*[2]

[1]*Department of Civil Engineering, High Institute of Engineering Technology, EL-Mina, Egypt*
[2]*Department of Civil Engineering, Sphinx university, Assiut, Egypt*

(Received April 15, 2022, Revised August 10, 2022, Accepted October 17, 2022)

Abstract. In spite of extensive testing of the individual shear wall and the coupling beam (CB), numerical and experimental researches on the seismic behavior of CSW are insufficient. As far as we know, no previous research has investigated the affectations of position of CB regarding to the slab level (SL). So, the investigation aims to enhance an overarching framework to examine the consequence of connection positions between CB and SL. And, three cases have been created. One is composed of the floor slab (FS) at the top of the CB (FSTCB); the second is created with the FS within the panel depth (FSWCB), and the third is employed with the FS at the bottom of the CB (FSLCB). And, FEA is used to demonstrate the consequences of various CB positions with regard to the SL. Furthermore, the main measurements of structure response that have been investigated are deformation, shear, and moment in a coupled beam. Additionally, wall elements are used to simulate CB. In addition, ABAQUS software was used to figure out the strain distribution, shear stress for four stories to further understand the implications of slab position cases on the coupled beam rigidity. Overall, the findings show that the position of the rigid linkage among the CB and the FS can affect the behavior of the structures under seismic loads. For all structural heights (4, 8, 12 stories), the straining actions in FSWCB and FSLCB were less than those in FSTCB. And, the increases in displacement time history response for FSWCB are around 16.1-81.8%, 31.4-34.7%, and 17.5% of FSTCB.

Keywords: ABAQUS; coupling shear wall system; ETABS; finite elements; rigid link; slab level; wall element

1. Introduction

The lateral deflections (LD) of a structure under seismic stresses are a major concern in mid to taller building design. This LD can be an essential indicator of the extent of structural damage. Also, it can cause unfavorable structure-structure interaction (i.e., pounding). Openings are frequently constructed in RC structural walls to suit aesthetic or other practical needs. The coupled shear wall (CSW) system that was employed extensively in modern taller buildings is regarded as the main lateral force-resisting system. Likewise, the CSW in conjunction with the CB had been functioned frequently in taller structures to raise lateral strength. The CSW system can endure a substantially base moment and shear force with significant increased structural stiffness in

*Corresponding author, Professor, E-mail: lamiaa.idriss@sphinx.edu.eg

http://www.techno-press.org/?journal=csm&subpage=8 ISSN: 2234-2184 (Print), 2234-2192 (Online)

comparison to the individual wall piers (WP) due to the effect of CB among the adjacent WP. Furthermore, during massive earthquakes, the CB has the ability to derive a substantial magnitude of energy and protect the WP from catastrophic damage. Several studies have undertaken extensive testing on the seismic behavior for numerous CBs (Lim *et al*. 2016, Wang *et al*. 2018, Galano *et al*. 2000, Singh *et al*. 2022, Ma *et al.* 2022, Tassios *et al*. 1996). Also, Yousufu Ma has researched how two steel plate shear wall piers interact with the coupling beams to improve the structure's capacity to overturn (Ma *et al.* 2022). In addition, two significant aspects must be considered in the design of the CSW: (1) During the test, the actual boundary conditions of the CBs in the CSW which include the constraints from adjacent WP and slabs, aren't easy to examine appropriately. Therefore, the realistic behavior of the CBs which is different from single beam specimen test ought to be investigated; (2) The appropriate ratio among diagonal and longitudinal bars in a hybrid-layout CB have to be ascertained depending on the assessment of system performance. Currently, structural simulation models with acceptable precision and efficiency are essential. And, they have to execute huge numbers of elastic-plastic dynamic THS analyses of numerous modeling to encourage and enhance research into structural seismic performance and performance-based design (Ding *et al*. 2018). Previous research must have shed the light on the design of the CBs to enhance their behavior by considering the material properties (Tian *et al.* 2019, Kumar *et al*. 2021, Kolozvari *et al.* 2018, Rezapour *et al*. 2022). Furthermore, two adjacent shear walls have been connected by a coupling beam made of a steel corrugated plate that has been employed on both of its sides (Zuo *et al.* 2022). However, slab stiffness has not been dealt with as a basic variable in the CB design to date. Nowadays, flat slab technique is widely employed in the construction where slab thicknesses are frequently bigger than other techniques. Consequently, it is appropriate to further assess the properties of this variable on the CBs in the flat slab. Neither the rigidity of the slab nor the effectiveness of the location of CBs regarding the SL is considered as fundamental variables in the designing of the CBs. Consequently, the paper is interested in developing a 3-d FE method to gain a better understanding of the studied cases' performance. Hence, the guidelines for constructing a stability system can be obtained. Considering the FE software (ETABS), a new combined beam-shell model of the CSW is formed with tremendous efficiency and exactness for the seismic examination. However, a time history (THS) analysis was done to calculate the THS reaction of the CB position during the future predicted earthquakes.

2. Literature review

The coupled shear wall (CSW) includes two RC wall pillars and multiple CBs where the CSW has a greater load-bearing capacity and lateral stiffness than individual WP because of the coupling effects of CBs (Ding *et al*. 2018). The CSWs are exceptional lateral load-bearing techniques that disperse inelastic deformation between CBs and WP. Multiple shear walls (SW) are preferred in load-bearing techniques because of their capacity to give redundancy and ductility to structures by dissipating energy via the creation of hinge zones. The connecting girders are vital in improving the seismic response of the double wall mechanism which can be the power dissipation source in the model. As well as, they can resist failure owing to the inherent transformation in stiffness. To sustain earthquake stresses, the connected SW mechanism should have high stiffness, strength, and power dissipation. Traditional reinforced CBs without diagonal bars (DBS), diagonal CBs with all longitudinal bars replaced with DBS, and hybrid-layout CBs with only part of the longitudinal bars replaced with DBS are the three sorts of CBs dependent on

reinforcement layouts. Although the diagonal CBs have a higher shear capacity, energy dissipation, and ductility than conventional CBs, its usage is severely restricted owing to construction challenges. As a result, a hybrid layout had been chosen to lesser significantly the difficulty of construction (Lim *et al.* 2016). In several design settings, structural walls are linked at each slab plate level by moment-resistant elements. In addition, stiff CBs or relatively flexible floor slabs have to be employed as connecting elements. The mutual reaction of the individual WP and the frame action arising from the linkage between WP and CBs can resist the lateral loads. Another key fact to remember is the degree of stiffness of the CBs to control the efficiency of the CSW. Owing to the CBs, the CSW acts as a composite cantilever with bending around the centroid axis of the wall groups. The verification of the overall response to powerful earthquakes is extremely difficult, especially because the positions of the walls deviate from the building's center of mass. However, the CSWs resist the overturning moment (OM) by a combination of an axial force couple that arises in the WPs. This is a result of the shear demand in CBs and flexural action in the WPs. Otherwise, the flexural stresses are resisted totally by the cantilever walls (Eljadei 2012). The coupling ratio (CR) is a function related to stiffness and strength for the beam and the wall. Similarly, the OM reaction by CBs is proportional to the (CR) degree. On the other hand, the CBs act as a fuse in the structural models to improve the resistance of the OM and thus creating the flexibility for dissipating energy (Aristizabal-Ocfaoa 1987). ACI 318-99 has recommended that the aspect ratio (AR) has to be fewer than four in the diagonal CB. Likewise, it is suggested to employ the transverse reinforcement round the DBS to resist the buckling effect. The slender CB with an AR of three is considered as familiar owing to the requirements of the architecture. However, the reduction in the aspect ratio of the DBS leads to a decrease in the effectiveness in shear resistance. Furthermore, a rise in the AR can produce an upsurge in the flexural that can cause the falling down of the structural members. So, it is needed for an alternative design like high-performance fiber carbon concrete. Similarly, this kind of RC concrete can allow the elimination of the DBS in addition to getting the same behavior of strength. As a reaction to the limited amount of experimental research, FEA emerges as a viable option to create the structural elements. At present, one-dimensional (1D) methods represent fiber beam components, truss elements and springs. Likely, the 1D method is the best appropriate tool to investigate the seismic behaviors of CSW. It could be suited to frame beams and columns where flexural behavior is dominant rather than the significant shear in the CSW mechanism (Lu *et al.* 2005, Santhakumar 1974, Álvarez *et al.* 2020). To date, it is a major gap in previous studies for the numerical methods of the CSW owing to the complex seismic reactions of CBs (Lu *et al.* 2005). As illustrated in Fig. 1, two simulation models ought to be abridged from past research where the WPs and CBs are represented using a complicated 2-D membrane component or a 3-D shell to achieve a higher accuracy. Fig. 1 depicts all previous modeling for creation the components of the CSW mechanism.

Two methods are designated for representing the CSW system:

First, the WPs and CBs are simulated by beam elements to improve computation efficiency as illustrated in Fig. 1(a). Second, the WPs and CBs are simulated using a complex 2D membrane or a 3D shell element to achieve improved precision as indicated in Fig. 1(b).

To put it another way, the 2D technique with high accuracy is more appropriate for planer CSW. However, there are 2D mechanism utilized insufficiently to simulate the CSW (Zhiwei *et al.* 2009).

Although, THS analysis is considered the most precise analysis for the structures confirmed to seismic actions (Harries *et al.* 2000). It would be more difficult than pushover analysis because of

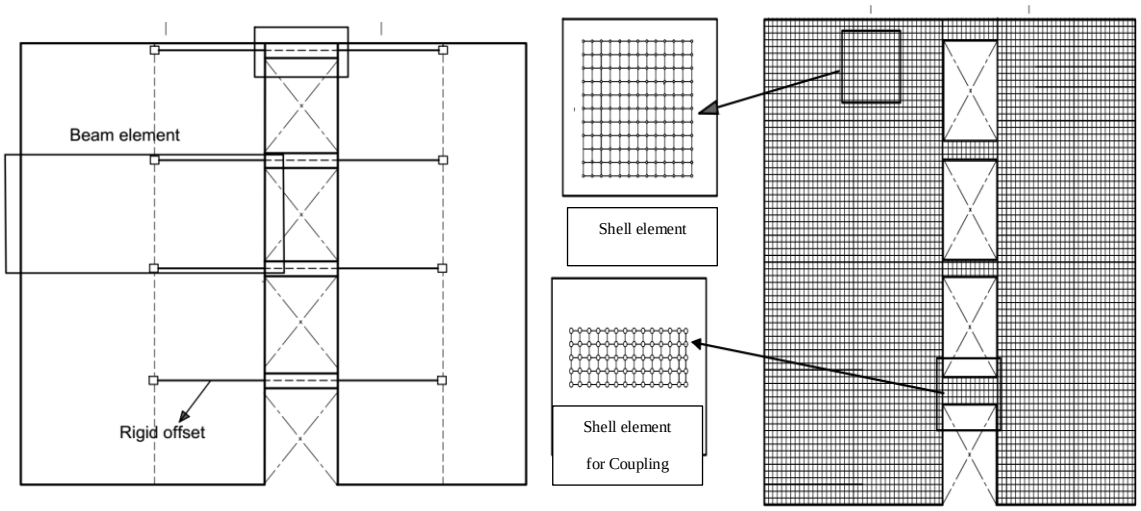

(a) Beam column element (b) Shell or membrane element

Fig. 1 Modeling methodologies for RC coupled wall system (Two approaches)

monitoring the cyclic inelastic behavior of structural members. What's more, the pushover analysis is a faster method that would provide a reliable assessment of the structure response. But, THS analysis methodology is the most accurate of all the dynamic methodologies. So, the thesis views THS analysis as the primary method for investigating CBs.

3. Finite element modeling

In order to perfect building structure geometry, a variety of three-dimensional (3D) modeling techniques have been employed, ranging from the approach for one-dimensional elements to detailed 3D solid modeling of all structural components. And, to effectively forecast a building's seismic response, an FE model is required to integrate all the structural elements and simulate their real behavior. Furthermore, creating these simulations typically takes more work. In general, this type of study has produced better results than simplified models. The results of this type of analysis have typically been better than those of simplified models. Analytical methodologies and models of variable complexity for structural buildings are developed to assess the various models' abilities to forecast the performance of CB as well as the implications of analysis assumptions on demand projections. On the other words, the modeling of the construction of the structure is done utilizing a comprehensive FE model that makes use of shell elements for the coupled beam, as shown in Fig. 2. Flexure dominates CB behavior and is best described using shell elements. And, quadrilateral shell pieces are used in this model to represent both the CB and the floor slab (Abdel Raheem *et al.* 2018). Therefore, the analysis takes into account how each member interacts in three dimensions. Three types of modeling have been created to investigate the different cases of CB positions. The first is made with FS at top of the CB (FSTCB). The second is created with FS within panel depth (FSWCB). And, the third is employed with FS at bottom of CB (FSLCB). On the other hand, the research simulates the CB and WPs using shell and wall elements.

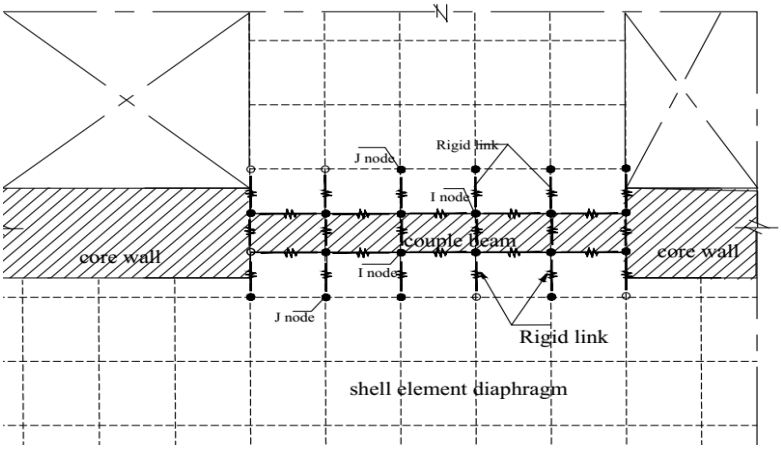

Fig. 2 Rigid link between coupled beam and the slab elements (Idriss *et al.* 2022)

Additionally, the rigid linkages (RLs) can be useful in creating stiffness linking models amongst them. On the other words, a new combined beam-shell model of the CSW is created for the seismic analysis with incredible efficiency and accuracy using the FE program (ETABS).

3.1 Rigid link between slab elements and coupled beam

The wall elements can be used to model CB and SW. Also, the rigid links (RLs) can be effective in developing models for rigidity linking between them. Besides, the RLs are a representative model in the FEM that states the kinematic interaction among the selected nodes. However, the RLs between numerous nodes are investigated by Fialko (2017). In most circumstances, the beam can indeed be denoted by simply attaching to the slab element's node which is incorrect and leads to the failure to express in-plane rotational stiffness (Idriss *et al.* 2022). As illustrated in Fig. 2, RL is among the strategies for creating the corrective model by transmitting the OM and shear force from the node shell element to others.

On the other hand, the stiffness of the shell elements can be impacted by the transfer of shear forces from the shell node to the inner nodes without rigid links. Therefore, the node I for all links is the node linked to the coupled beam node. The end that extends into the nodes of the slab elements is known as node *J*. All rigid links' *J* ends should have their degrees of freedom *x*, *Mx*, *My*, and *Mz* released. From the J end to the inside shell elements node, only the Y and Z degrees of freedom should be connected. The shear forces can be transferred from slab elements into a coupled beam using this release configuration. Additionally, the presence of the rigid connection won't have a negative impact on the rigidity of the shell element.

4. Proposed mixed beam-shell model for RC coupled walls

Even in the elastic range, bending deformations in a deep coupling panel are minimal. And, the majority of the deformation is due to shear. As the depth of the CB decreases, they become more critical and may require modeling. When there are significant bending deformations, wall elements should be functioned in representing modeling. Consequently, shell and wall elements are utilized

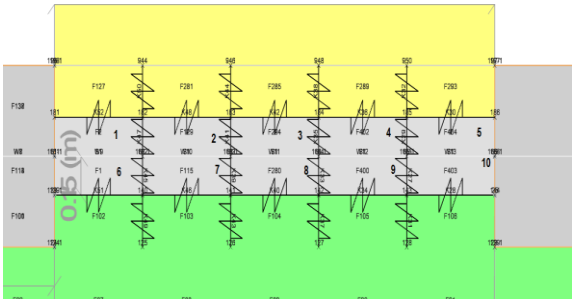

No of shell element for coupled beam (Configuration Plan)

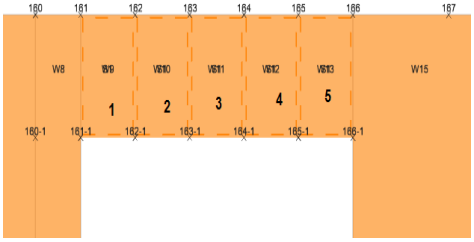

No of shell element for coupled beam (Elevation) (Case1)

Fig. 3 No of shell elements

to simulate the CB and WPs in the research. The CB has at least five meshes running the length of it. In addition, the set of coupling wall elements have the similar number of the slab elements connected to the coupling wall element. Fig. 3 displays RL linking between elements. The sum of meshes in Y–direction is two meshes. As well as, the count of shell elements ranges from one to two in the direction of the CB height.

5. Modal response spectrum (RS) method

The RS mechanism is applicable to all kinds of structures where the involvement of the model in each orthogonal direction exceeds ninety percent of the mass of the structure. In addition, the count of vibration modes established by FE modeling are bigger than ninety percent from mass involvement. On the other hand, the ASCE 7-10 code standards are utilized with the assumption response modification factor R=5 and soil type C for estimating the lateral seismic design loads on the buildings (Engineers 2000). Furthermore, the soil class 'C' states the dense and stiff soil. And, the seismic region chosen for this research is zone 5B per the Egyptian code. Self-weight, floor cover, and 25% of the live load are all included in the total seismic mass. And, the curve of the spectrum is type 2 (The seismic region parameter and importance factor are equal to 0.3 and 1, respectively). As well, section 12.8 of ASCE 7-10 is used to calculate earthquake loads. Following are the steps to compute the seismic base shear V (Engineers 2000)

$$V=C_s W \tag{1}$$

Where, W is the effective seismic weight and C_s is the seismic response coefficient.

$$C_s = \frac{S_{DS}}{\frac{R}{I_e}} \tag{2}$$

Where, S_{DS} refers for the design spectral response acceleration for 5% damping, I is the importance factor, and R is the response modification factor.

The calculated seismic response coefficient must not be more than:

$$C_s = \frac{S_{D1}}{T(\frac{R}{I_e})} \qquad For\ T \leq T_L$$

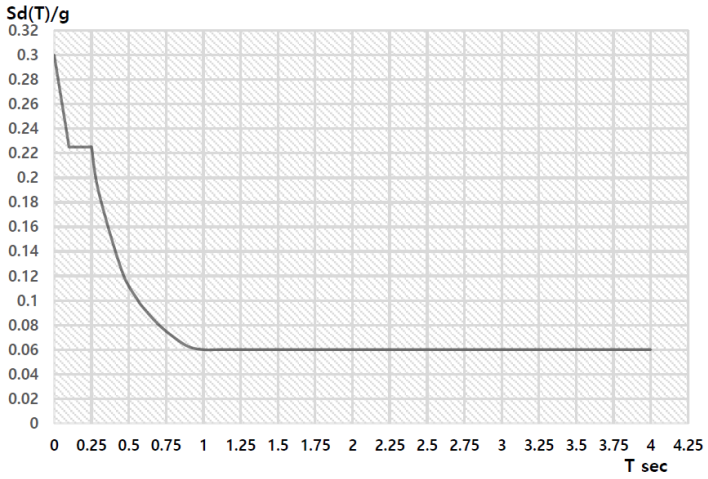

Fig. 4 RS curve

And

$$C_s = \frac{S_{D1}T_L}{T^2(\frac{R}{I_e})} \qquad For\ T > T_L$$

Where, T is the structure's fundamental period, T_L is the long-period transition period, and S_{D1} is the design spectral response acceleration value at a period of 1.0 s. On the other hand, the mapping risk-targeted maximum regarded earthquake spectral response acceleration factors are used to establish the design earthquake spectral response acceleration factors at a short period and at 1 s period. The *RS* curve is illustrated in Fig. 4.

In the response spectrum approach, the directional combination is made using the square root of the sum of the squares (SSRS), and the modal combination is made using the complete quadratic combination (CQC). In order to determine the key aspects of the dynamic behavior of the building, a three-dimensional numerical model of the physical structure is employed to depict the structure's mass and stiffness distribution.

6. Selected input ground motions

The position of the CB with respect to the SL is implemented in three dimensions. And, its impacts on the seismic reactions are investigated for Corralitos ground shakings where Corralitos Earthquake THS data is defined by California state (USA). Furthermore, the peak ground acceleration is determined by 618 cm/s^2 for north-south direction. Fig. 5 displays the THS reaction for Corralitos Earthquake. Furthermore, the goal of the research is to recognize the optimal location of the CB relying on seismic behavior decline.

7. The cases of studies

Upon the FE software, a new composite beam-shell model for CW seismic analysis is

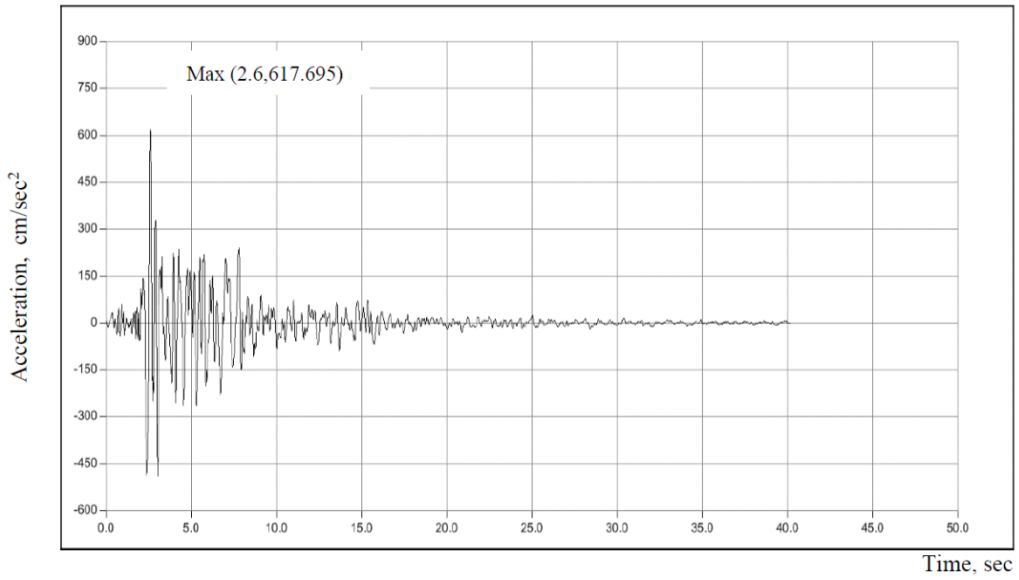

Fig. 5 THA for Corralitos earthquake

functioned with sufficient efficiency and precision. The behavior of CB position is presented in 3-D models. The four, eight, and twelve-story finite element models based on a 3D constitutive model are suggested and examined. The response assessments are evaluated for several models of building (4, 8, and 12 stories). As indicated in Fig. 6, three cases are created. The first is made with FS at top of the CB (FSTCB). The second is created with FS within panel depth (FSWCB). And, the third is employed with FS at bottom of CB (FSLCB).

8. Objectives of research

The mentioned work aims to decide the optimal CB position in relation to the SL for lateral load resistance. Different models 4, 8, 12 stories are studied to evaluate the structural response of the building in relation to the position of CB. The current research seeks to give designers a clear vision about the location of CBs. Moreover, the overall response of the CB along the construction height under the seismic behavior is investigated to get the effect of the location of CBs. Besides, THS analysis are conducted to determine displacement and acceleration THS responses.

9. Mathematical modelling

Three structural models (Four, Eight, and Twelve stories) are studied to implement the essential analysis and hence obtain the guidelines. An initial design approach is conducted to estimate the dimensions of the construction elements. The self-weight and the flooring loading are included in the dead loads. For every level, the flooring load (FL) is one and half Kn/m^2, and the live load (LL) is two and half Kn/m^2. The height of the structural modeling is 3.60 m. Fig. 6 demonstrates the configuration of modeling. To keep things simple, the construction area (20.87 m×23.52 m)

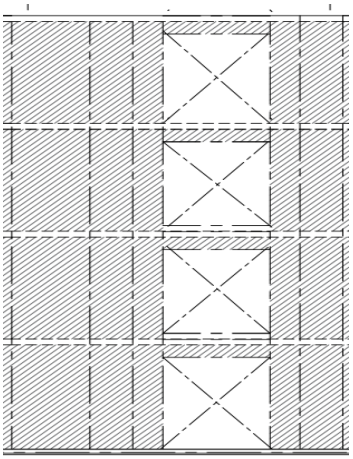

(Case 1) floor slab (FS) at top of (CB)

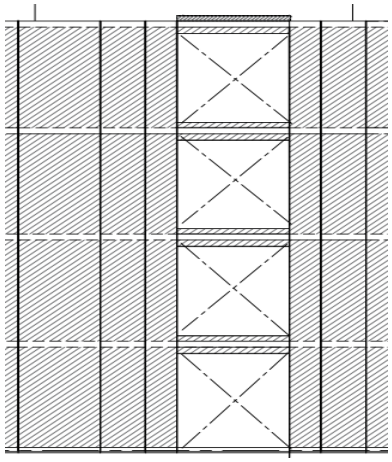

(Case 2) floor slab (FS) within panel depth (CB)

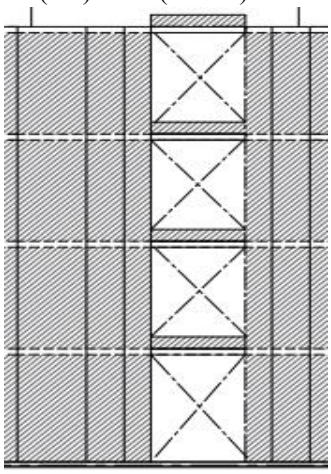

(Case 3) floor slab (FS) at bottom of CB

Fig. 6 Cases of studies

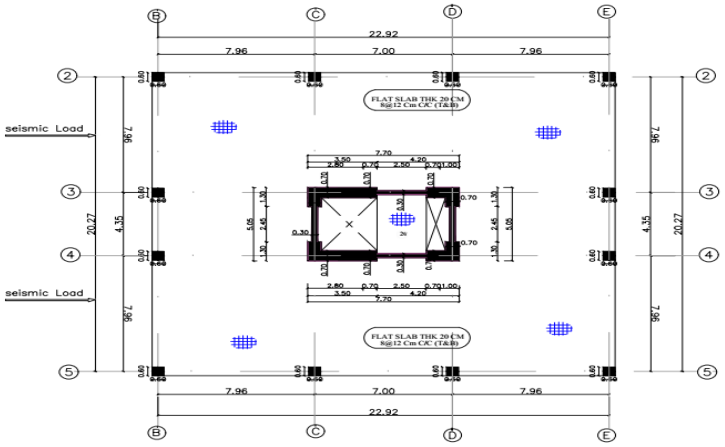

Fig. 7 Configuration plan

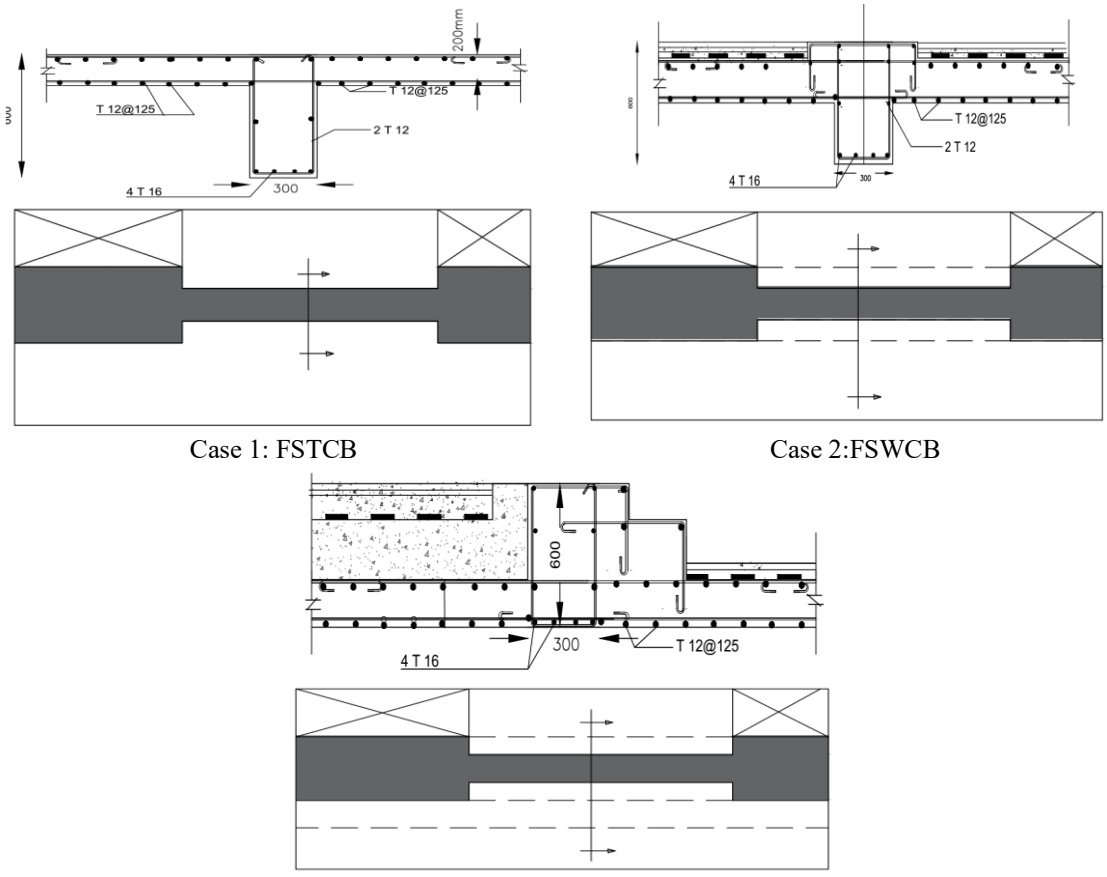

Case 1: FSTCB Case 2:FSWCB

Case 3:FSLCB

Fig. 8 The details of the coupling beam with different cases (1,2,3)

as exposed in Fig. 7 is identical for the whole stories. The dimensions of the cross-section of the columns employed as an initial design are 60 cm×60 cm. Moreover, all slabs have the same thickness with a value of twenty centimeters, and all elements are designed to be safe in accordance with ACI 318 (Committee *et al.* 2020). As a result, the features of the CB cross-sections are depicted in Fig. 8. The concrete compressive strength C45 equates 45 MPa. And the yield strength of steel type ST40/60 is determined by 400 MPa. In addition, the poisson ratio of steel is 0.3.

Fig. 9 shows the methodology of research. It contains the goal of research for evaluating the response for different cases of CB position. Furthermore, it comprises two methods for analysis: the response spectrum and time history analysis. As a result, the values of main measurements are obtained. Where, lateral displacement and straining actions have been analyzed first method. And, the second method have been used to measure displacement and acceleration of time history analysis. In final of research, the CB mechanism is simulated to further understand the implications of slab position states on the CB rigidity. And, ABAQUS are functioned to figure out the stress distribution, shear stress criterion (Tresca yield criterion (S)), displacement(U), and strains (Logarithmic strain (LE)) for four stories.

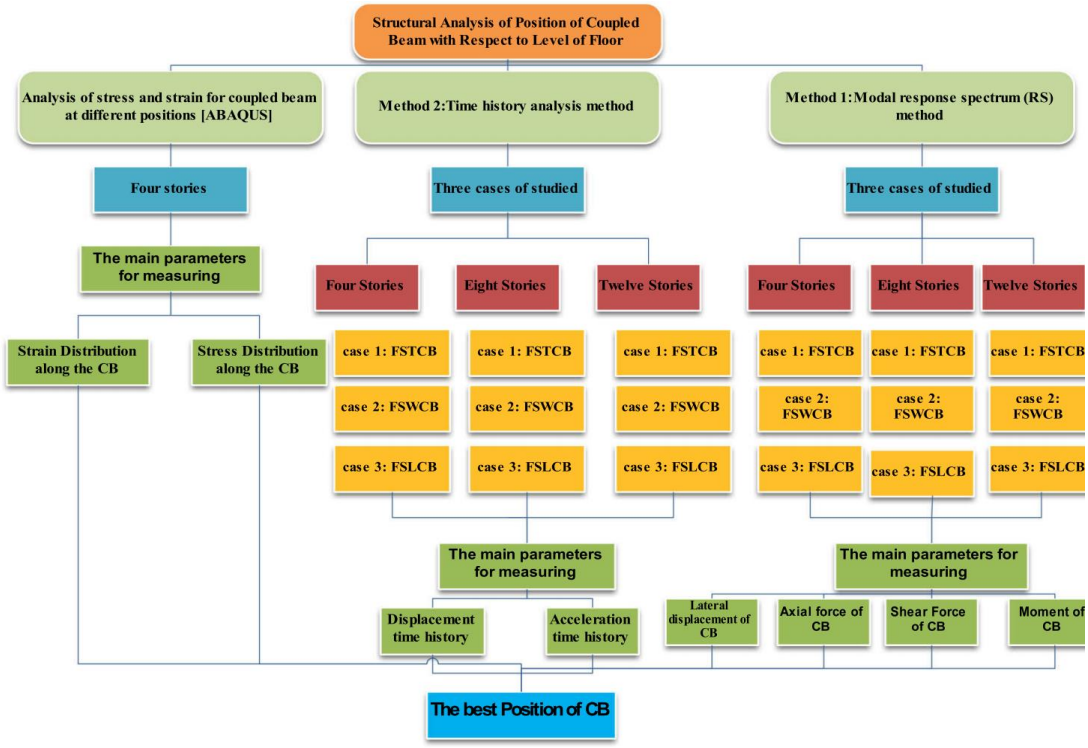

Fig. 9 Methodology flowchart

10. Numerical results and discussion

To determine the optimal performance, this study work assesses the effects of the coupled beam position on the response demands. The lateral displacements and straining actions may be significantly impacted due to CB's various positions with respect to SL. And, these important factors can analyze how each point behaves along a coupled beam's structural element. Furthermore, the variations between these measurements could change the level of performance of the structure's building. Hence, the maximum stress and strain can then be calculated at each place on the CB structure member.

On the other hand, the factor most frequently linked to the intensity of ground motion is peak ground acceleration. However, it is now commonly recognized that this is a criterion for determining the potential for damage. And, a significant peak acceleration could be connected to either a short-duration (high-frequency impulse) or a long-duration (low-frequency impulse). On the other hand, the structure's displacement response is defined by cycles with significant displacement amplitudes linked to the massive pulse in the input ground motion. Therefore, the study had been interested to investigate both the displacement and acceleration time history analysis.

10.1 Lateral Displacement Ux (Response Spectrum in X direction)

The rigidity linking between CB and slab elements has a tremendous impact on the behavior of

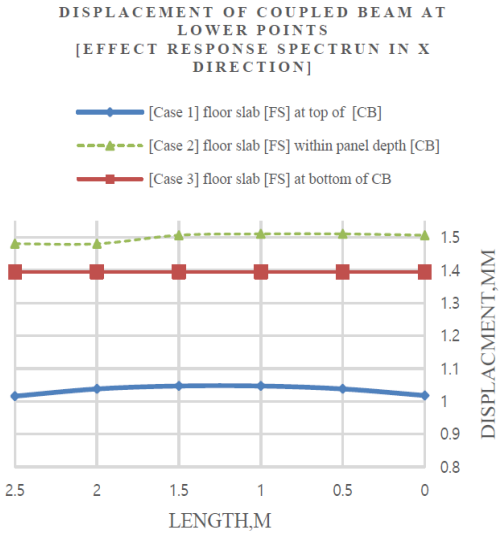

(a) Ux of the CB at LWE

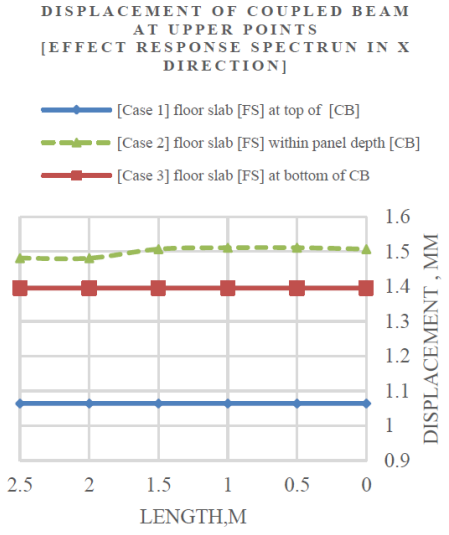

(b) Ux of the CB at UPE

Fig. 10 Ux of the CB (Four stories)

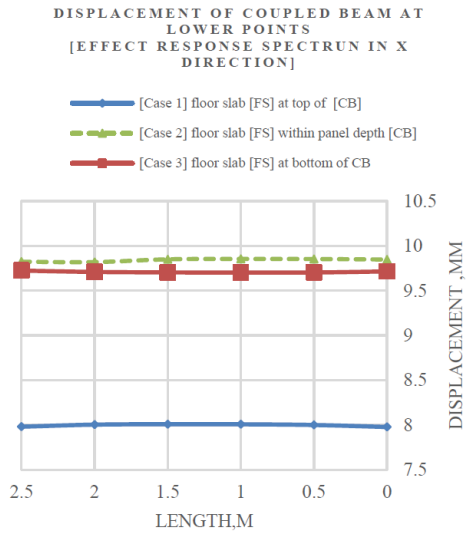

(a) Ux of the CB at LWE

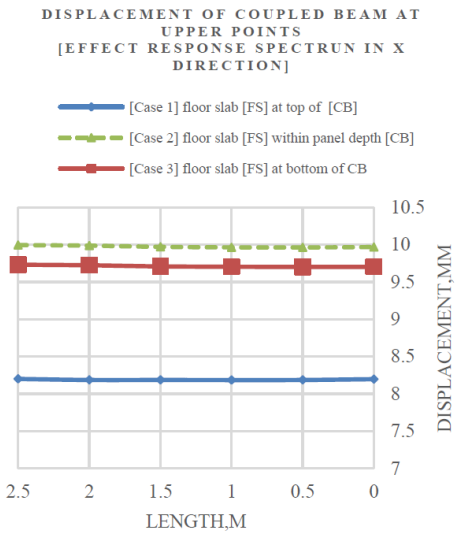

(b) Ux of the CB at UPE

Fig. 11 Ux of CB (Eight stories)

the CB under seismic loading (Idriss *et al.* 2022). Figs. 10-12 show the effects of connection positions between the CB and the SL on the LD for various cases (1-2-3).

The results demonstrate the variations among the studied cases ((case 1: FSTCB), (case 2: FSWCB), (case 3: FSLCB)), the outcomes indicate that:

For four stories: the percentage of the increase in lower wall elements (LWE) of the CB for (case2: FSWCB) and (case3: FSLCB) compared to (case1: FSTCB) are 42.68% and 37.30%, respectively. Besides, the increasing percentages in the LD are 39.19% and 31.13% for the upper

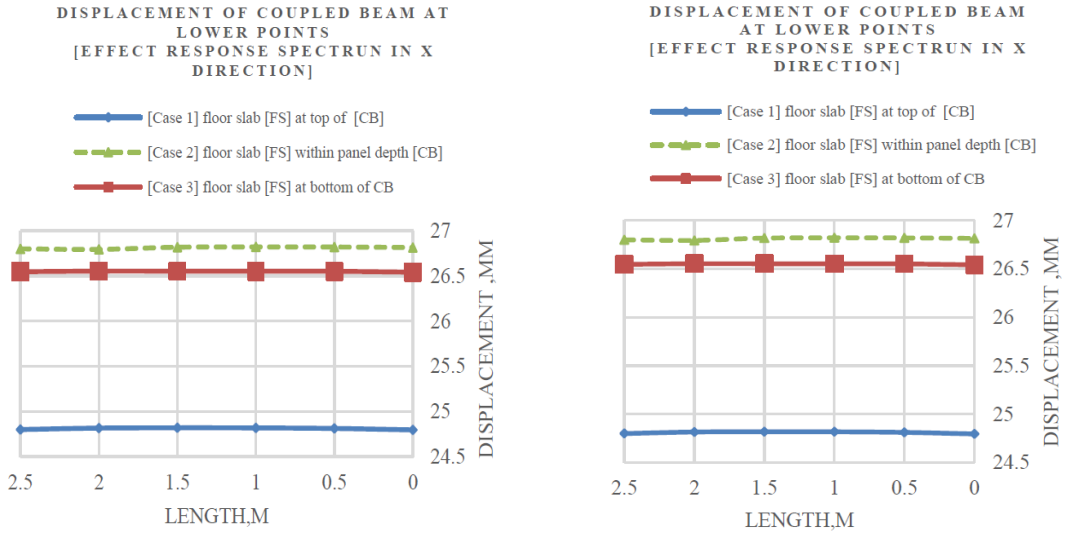

(a) Ux of the CB at LWE (b) Ux of the CB at UPE

Fig. 12 Ux of the CB (Twelve stories)

wall elements (UWE) as presented in Fig. 9.

For eight stories: the percentage of the increase in LWE of the CB for (case 2: FSWCB) and (case3: FSLCB) regarding (case1: FSTCB) are 22.66% and 21.83%, respectively. In addition, the increasing percentages in the LD are 21.59% and 18.78% for the UWE as demonstrated in Fig. 10.

For twelve stories: the percentage of the increase in LWE of the CB for (case 2: FSWCB) and (case3: FSLCB) with respect to (case1: FSTCB) are 7.97% and 7.04%, respectively. Also, the increasing percentage are 7.27% and 6.36% for the UWE as revealed in Fig. 11.

10.2 Straining action of CB (Response Spectrum in X direction)

For the studied cases, the analysis shows that there is a variation between values of axial forces, shear, and moment on the CBs running the heights of the model. Fig. 13 to Fig. 15 display the deviation path between values, which indicates the reducing of values of straining action (Axial force, Shear, Moment). This is a result of the position of rigidity connection between the CB and the slab level. Moreover, Figs. 13,14, and 15 show the percentages of reducing straining actions for (case2: FSWCB) and (case3: FSLCB) compared to (case1: FSTCB). The reduction percentages for axial forces, shear, and moment display that:

For four stories:

Axial force: (case 2: FSWCB) in comparison with (case 1: FSTCB): the range of decreasing is between -95.9% to -83.9%. (case 3: FSLCB) concerning (case 1: FSTCB): the range of decreasing is between -61.2% to -12.9%.

Shear force: (case 2: FSWCB compared to (case 1: FSTCB): the range of decreasing is between -46.8% to -38.9%. (case 3: FSLCB) regarding (case 1: FSTCB): the range of decreasing is between -37.3% to -26.6%.

Moment: (case 2: FSWCB) in contrast to (case 1: FSTCB): the range of decreasing is between -28.9% to -6.5%. (case 3: FSLCB) in relation to (case 1: FSTCB): the range of decreasing between

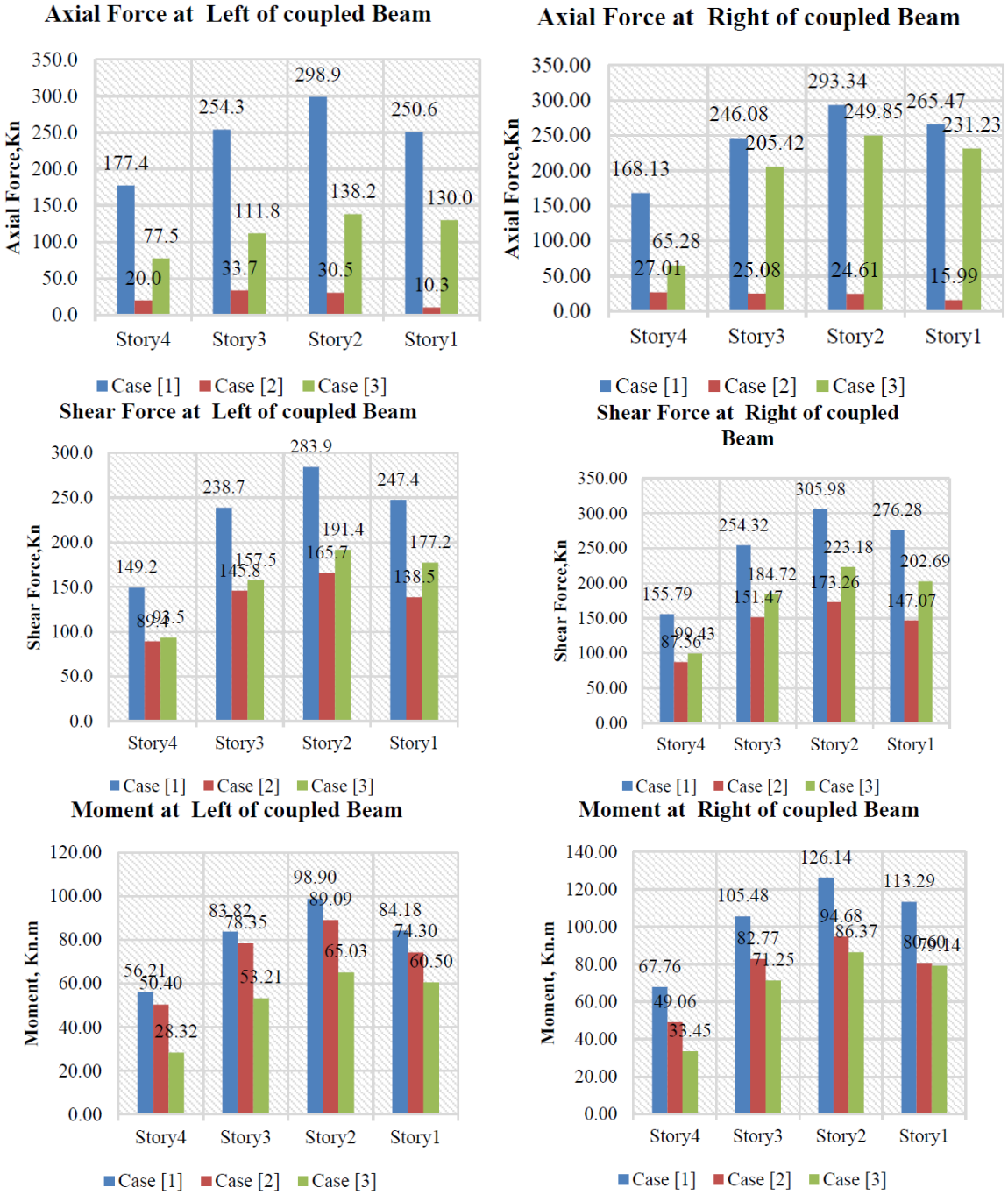

Fig. 13 Straining actions of the CB (four stories)

is -50.6% to -30.1%.

For eight stories:

Axial force: (case 2: FSWCB) in comparison with (case 1: FSTCB): the range of decreasing is

Fig. 14 Straining actions of the CB (Eight stories)

between -97.4% to -64.1%. (case 3: FSLCB) in contrast to (case 1: FSTCB): the range of decreasing is between -92% to -13.8%.

Shear force: (case 2: FSWCB) in relation to (case 1: FSTCB): the variation of decreasing is

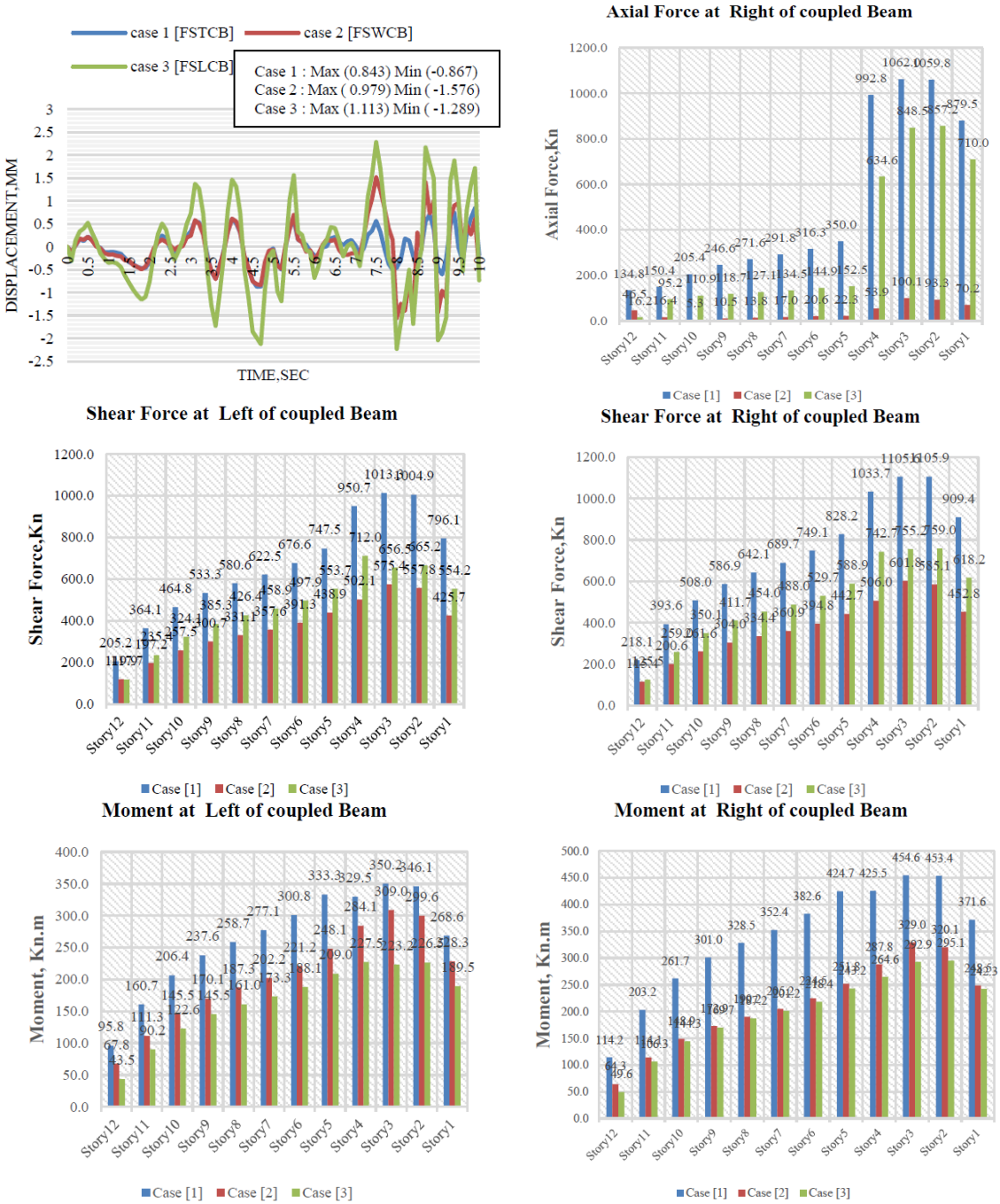

Fig. 15 Straining actions of the CB (Twelve stories)

between -48.3% to -36.7%. (case 3: FSLCB) concerning (case 1: FSTCB): the variation of decreasing is between -38.3% to -21.3%.

Moment: (case 2: FSWCB) regarding (case 1: FSTCB): the range of decreasing is between -

39.3% to -6.9%. (case 3: FSLCB) compared to (case 1: FSTCB): the range of decreasing is between -53.2% to -25.2%.

For twelve stories:

Axial force: (case 2: FSWCB) in comparison with (case 1: FSTCB): the range of decreasing is between -97.4% to -65.2%. (case 3: FSLCB) compared to (case 1: FSTCB): the range of decreasing is between -94% to -19.1%.

Shear force: (case 2: FSWCB) in relation to (case 1: FSTCB): the range of decreasing is between -51.0% to -41.3%, (case 3: FSLCB) regarding (case 1: FSTCB): the range of decreasing is between -42.7% to -25.1%.

Moment: (case 2: FSWCB) concerning (case 1: FSTCB): the variation of decreasing is between -43.9% to -11.8%, (case 3: FSLCB) in relation to (case 1: FSTCB): the variation of decreasing is between -56.6% to -29.5%.

Displacement and acceleration time history:

The cases of position (cases: One, Two, three) are analyzed to realize the affections of the position of rigidity linkage amidst the SL and the CB on the seismic performance. The three-dimension models are utilized, and, dynamic calculations are conducted by applying effective ground shaking acceleration at the base. The last results illustrate the LD and acceleration of the THS at the connection point (at the top floor) among the CB and the SF. Furthermore, the investigations disclose that the positions of rigidity linkages have an impact on the acceleration and displacement of the THS behavior because of variations in stress and strain distributions on the CB depth. Figs. 16 and 17 show LD and an acceleration of the THS for the studied cases.

Regarding the studied cases: the increases in displacement THS response related to (case 2: FSWCB) of CB positions for four, eight, and twelve stories are around 16.1-81.8%, 31.4-34.7%, 17.5% of (case 1: FSTCB). What's more, the increasing percentages in (case 3: FSLCB) in relation to (case 1: FSTCB) are 32-48.7%,7.5%,10.8-18.4%, respectively. Regarding acceleration THS analysis, the percentages of increasing of acceleration of the THS for (case 2: FSWCB) compared to (case 1: FSTCB) are in the range of 38% to 47% for eight stories as indicated in Fig. 17. However, the measures of decreasing for (case 3: FSLCB) with respect to (case 1: FSTCB) are about 49.6-19.5% for four stories. On contrary, in case of twelve stories, the percentage of raising acceleration of the THS for (case 2: FSWCB) and (case 3: FSLCB) in comparison to (case 1: FSTCB) is 24% as plotted in Fig. 17(c). Besides, the placements of the CB have an extensive effect on the THS due to the place of stiffness connection as shown in Figs. 16 and 17. Furthermore, the outcomes of the stress and strain variations alternate depending on the places of linking connections between the CB and the SL.

The response along the coupling beam for construction building:

The maximum and minimum response of the CB over the models' heights have a discrepancy in values due to the linkage position among the CB and the SL. Fig. 18 to Fig. 23 illustrate that the maximum and minimum values for the shear and moment under an effective earthquake motion alternate regarding different cases. What's more, the best state for lessening the shear values in eight and twelve stories is (case 2: FSWCB). As well as, the finest option for the lowering the maximum and minimum moment measurements is (case 3: FSLCB). Furthermore, a noteworthy solution for the linking position is the FS at top of the CB in four stories.

The CB mechanism is simulated to further understand the implications of slab position states on the CB rigidity. ABAQUS (Abaqus *et al.* 2001) are functioned to figure out the stress

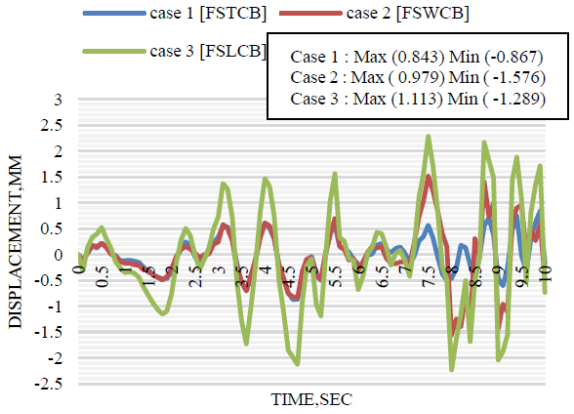

(a) Four stories

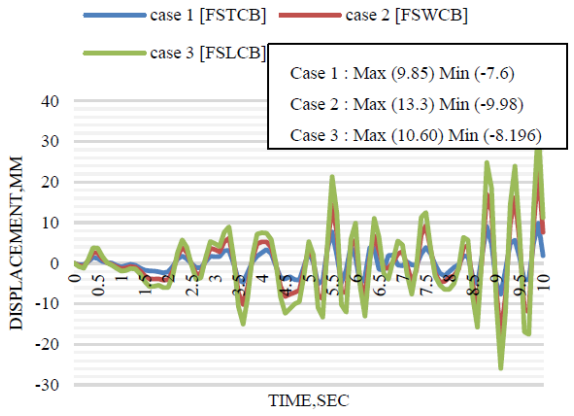

(b) Eight Stories

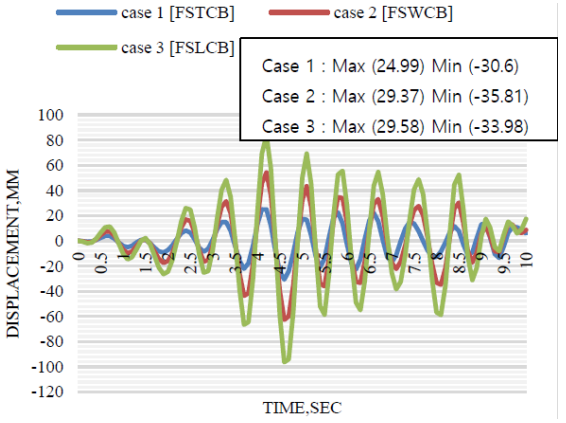

(c) Twelve Stories

Fig. 16 Displacement THS at connection point (the top floor) between the CB and the SF

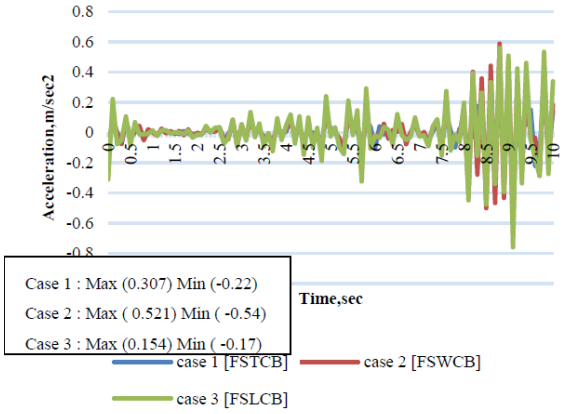

(a) Four stories

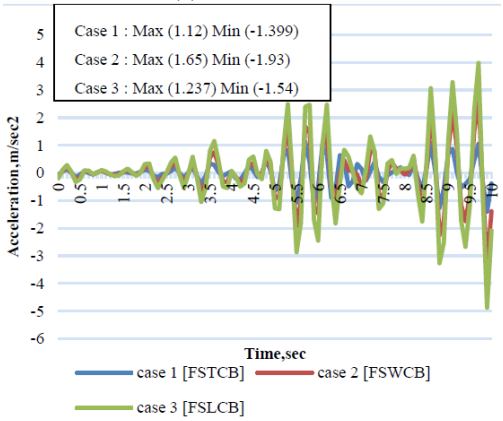

(b) Eight Stories

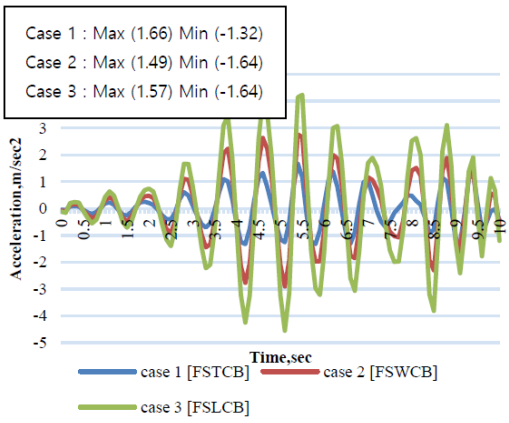

(c)Twelve Stories

Fig. 17 Acceleration THS at connection point (the top floor) between the CB and the SF

distribution, shear stress criterion (Tresca yield criterion (S)), displacement (U), and strains (Logarithmic Strain (LE)) for four stories. Where, the maximum shear stress theory serves as the

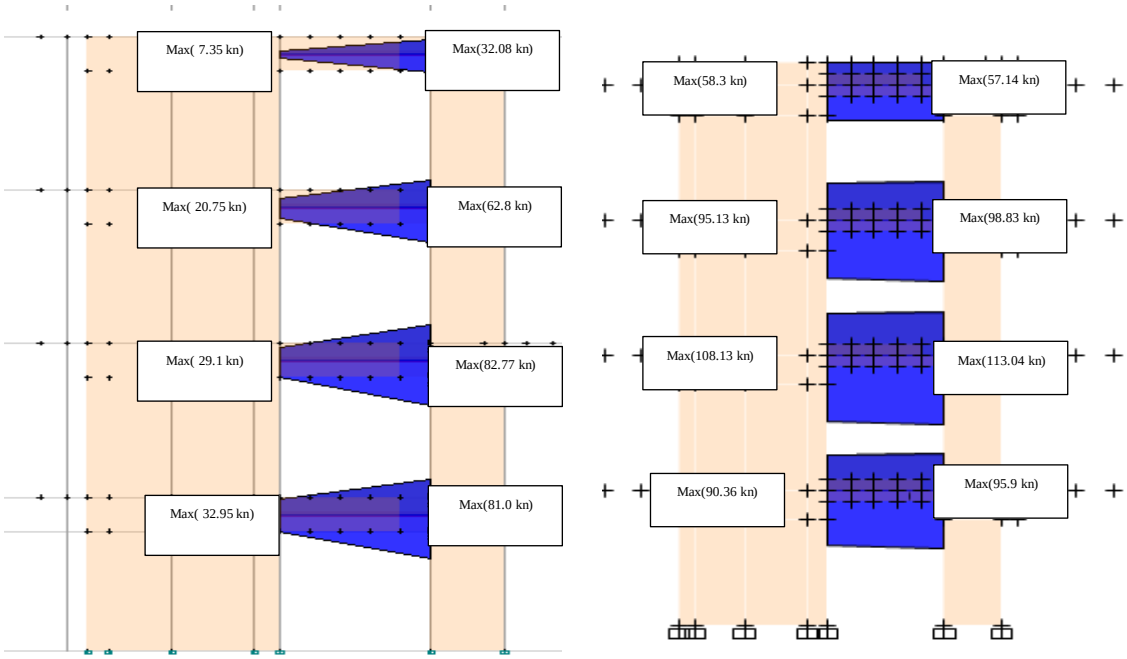

case 1 (FSTCB) case 2 (FSWCB)

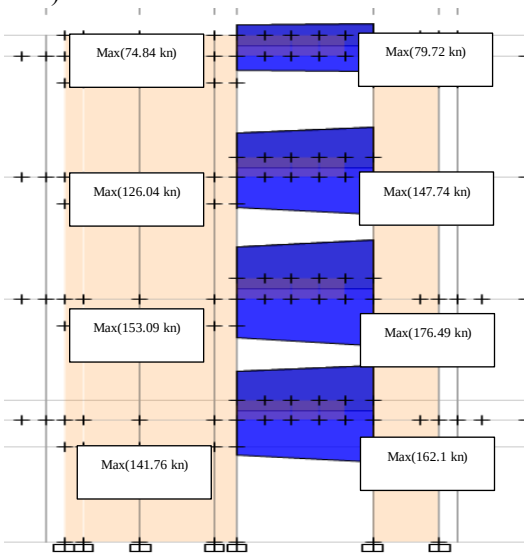

case 3 (FSLCB)

Fig. 18 The min and max shear response of the CB over the model heights (4 stories)

foundation for the maximum shear stress criterion, sometimes referred to as the Tresca yield criterion. According to this theory, a material will fail when the absolute maximum shear stress reaches the stress at which it yields in a straightforward tension test. According to maximum principal stress, a material fails when its principal stress as a result of any loading is higher than

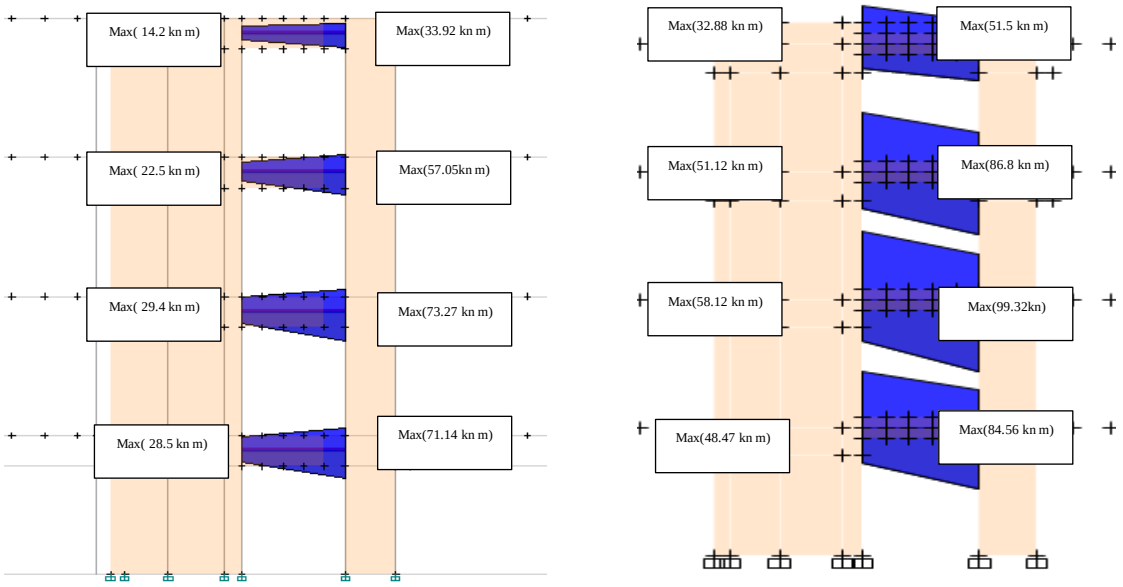

case 1 (FSTCB) case 2 (FSWCB)

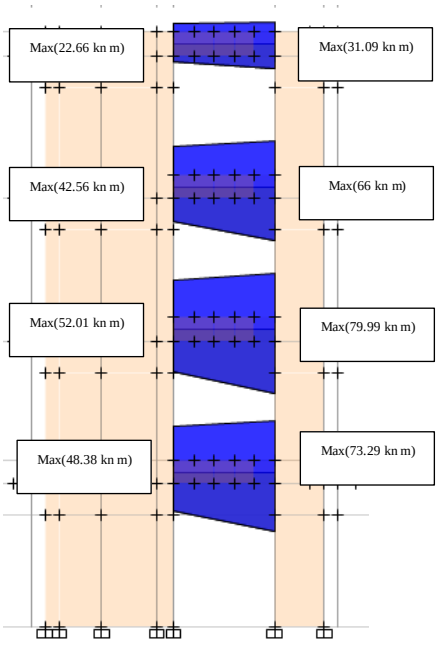

case 3 (FSLCB)

Fig. 19 The min and max moment response of the CB over the heights of models (4 stories)

the principal stress at which the failure takes place (Abaqus *et al.* 2001). Figs. 25, and 26 display the stress and strains variations for the CBs in four stories. The shell and walls elements are employed for more accuracy to simulate the CBs and the WPs as simulated in Fig. 24.

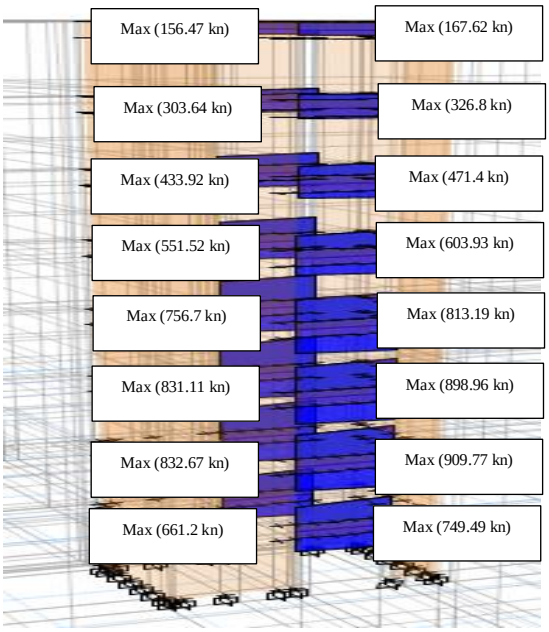

case 1 (FSTCB)

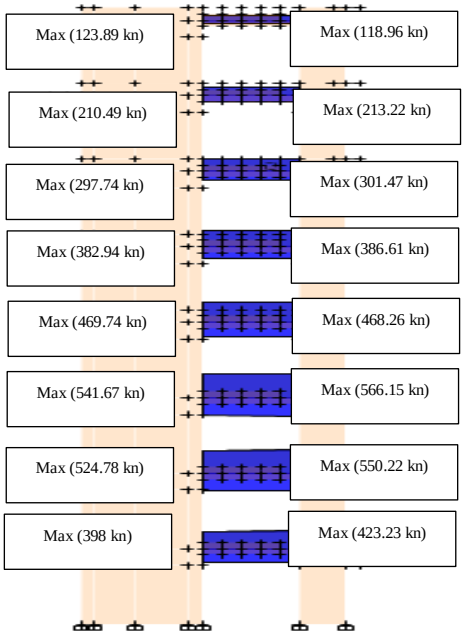

case 2 (FSWCB)

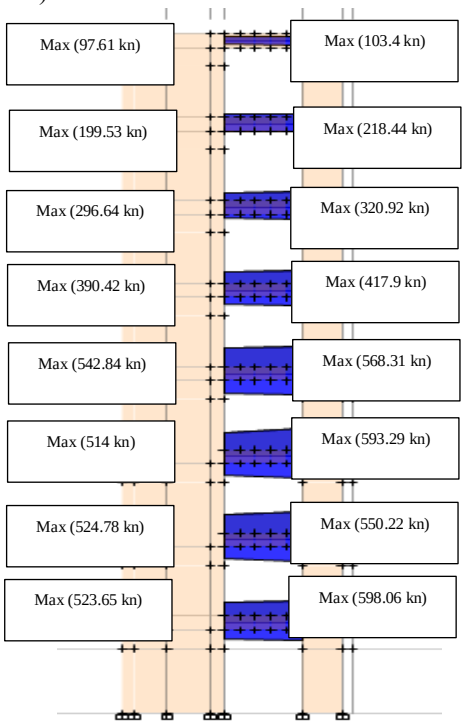

case 3 (FSLCB)

Fig. 20 The min and max shear response of the CB over the model heights (8 stories)

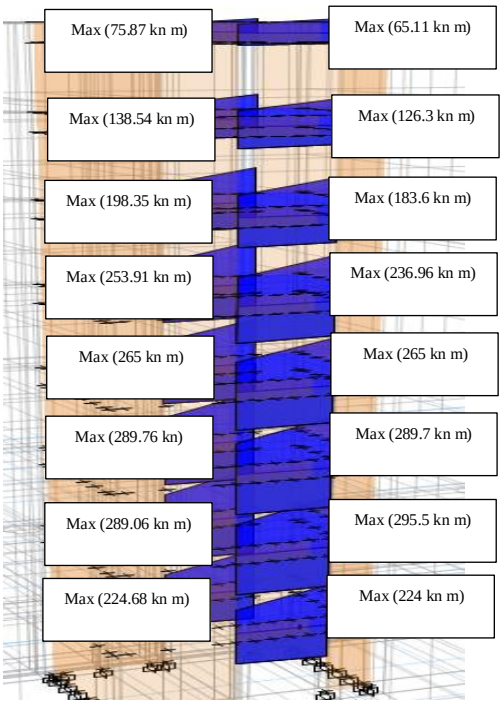

case 1 (FSTCB)

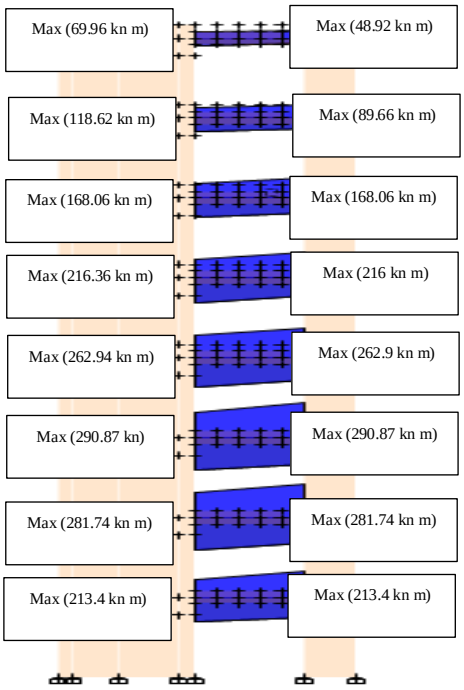

case 2 (FSWCB)

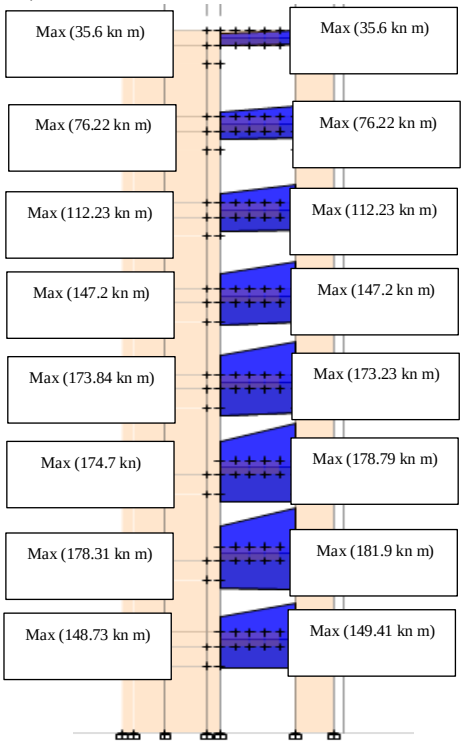

case 3 (FSLCB)

Fig. 21 The max and min moment response of the coupled beam along the building (8 stories)

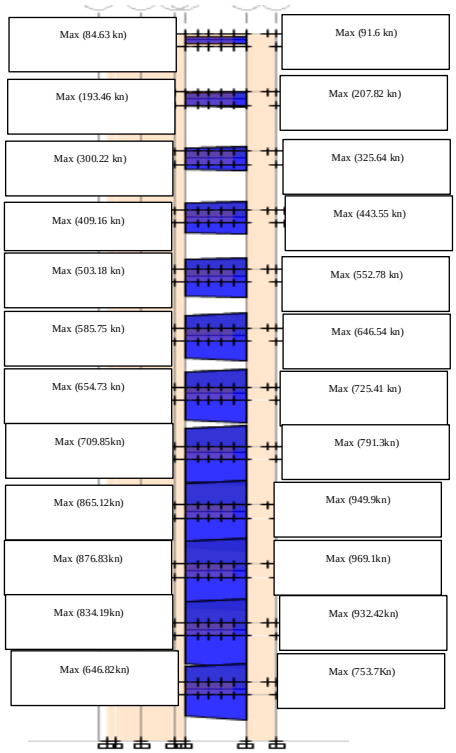

case 1 (FSTCB)

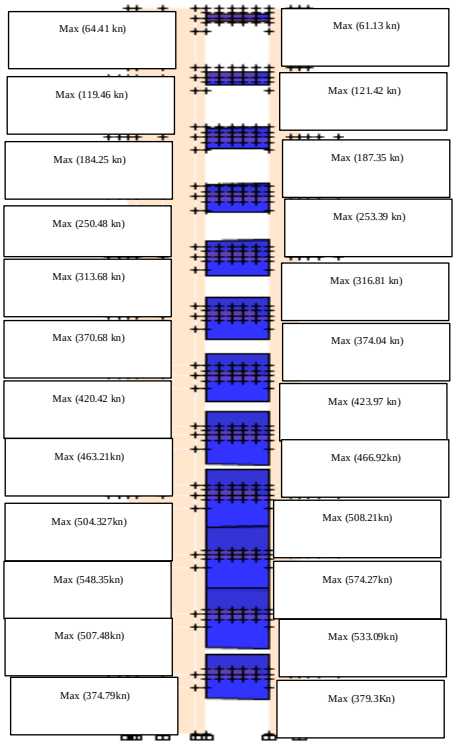

case 2 (FSWCB)

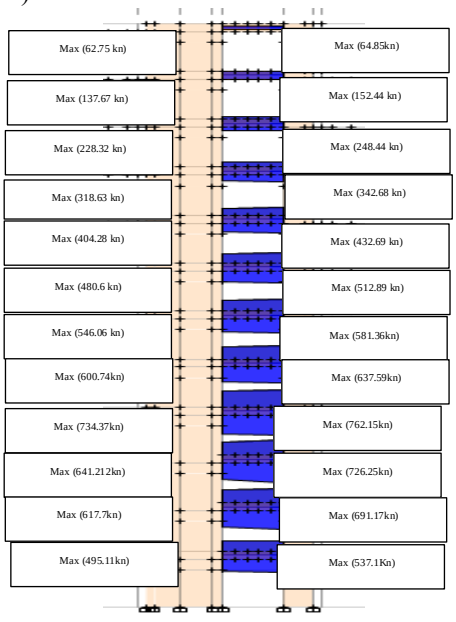

case 3 (FSLCB)

Fig. 22 The min and max shear response of the CB over the model heights (12 stories)

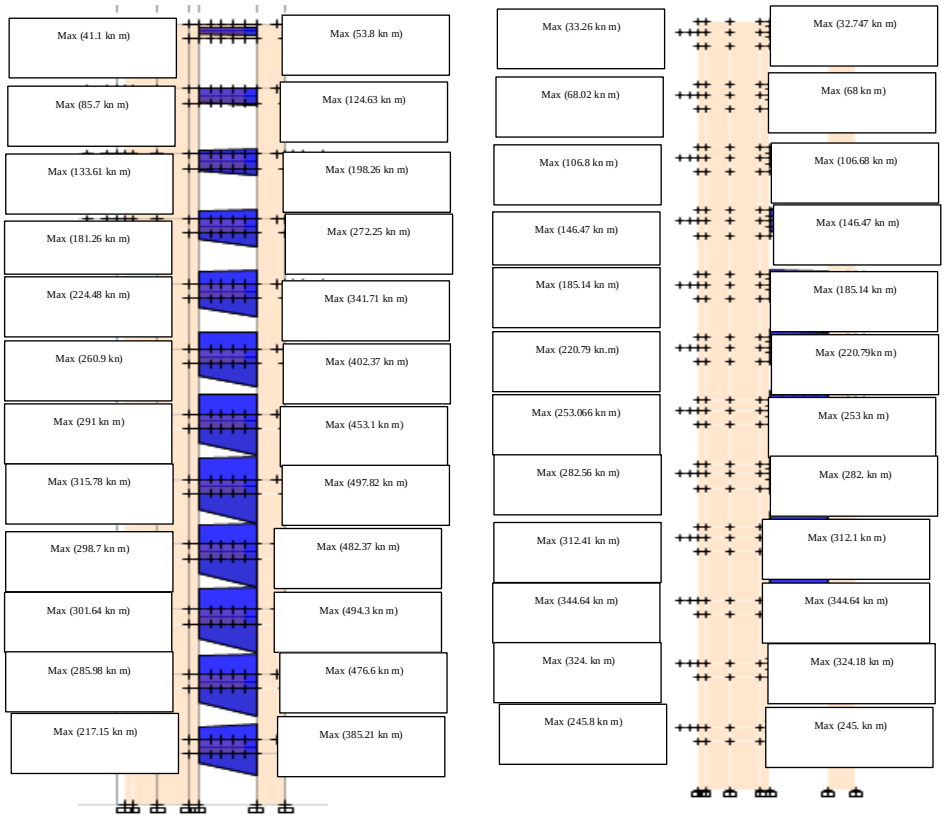

case 1 (FSTCB) case 2 (FSWCB)

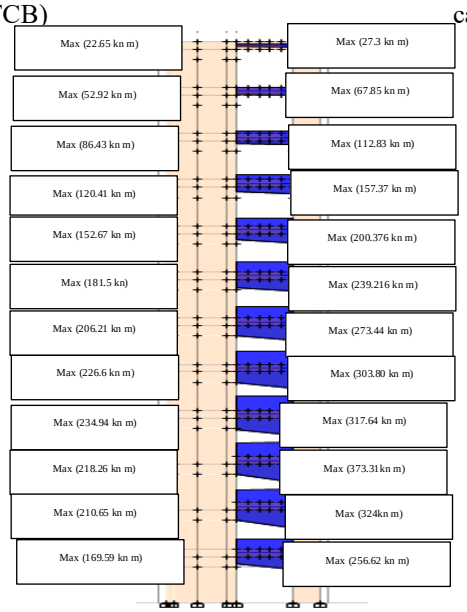

case 3 (FSLCB)

Fig. 23 The min and max moment response of the CB over the heights of models (12 stories)

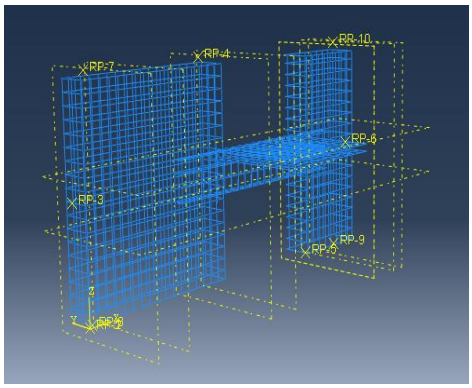

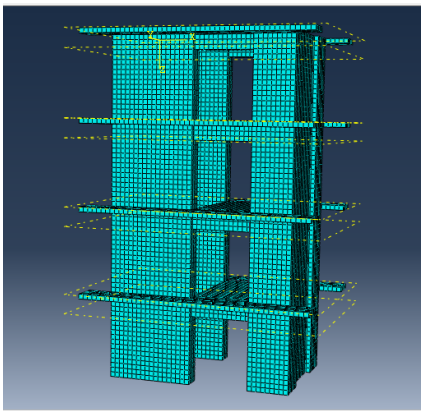

Beam-Shear wall reinforcement and slab connection Mesh element for coupling beams and shear walls

Fig. 24 Mesh elements for coupling beams and shear walls, the reinforcement for CB and SW

The maximum principal stress Tresca Shear stress

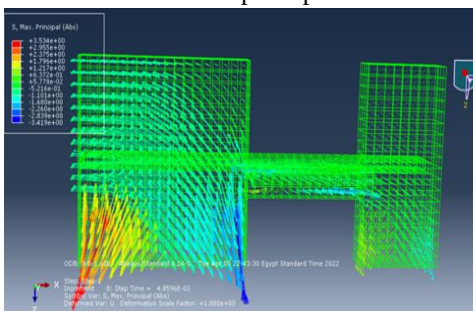

(FSTCB)

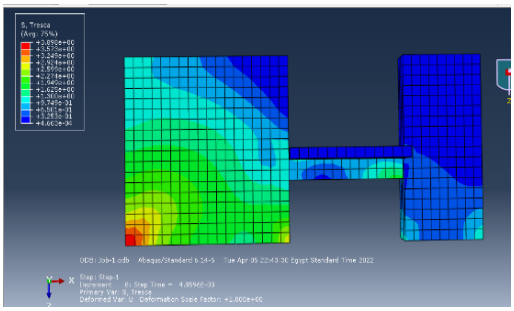

(FSTCB)

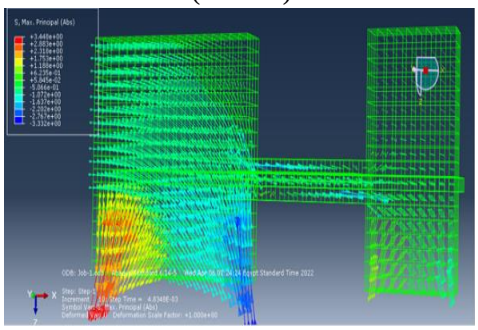

(FSWCB)

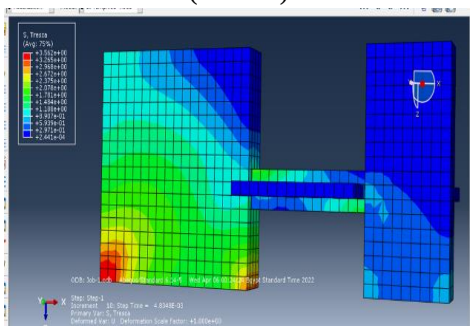

(FSWCB)

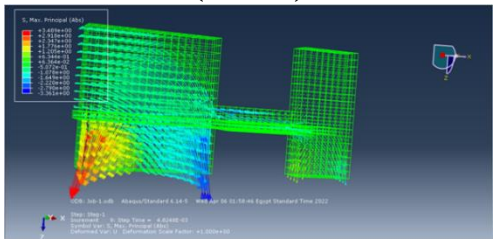

(FSLCB)

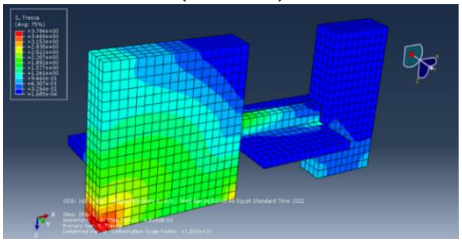

(FSLCB)

Fig. 25 The max principal stress and Tresca shear stress for four stories

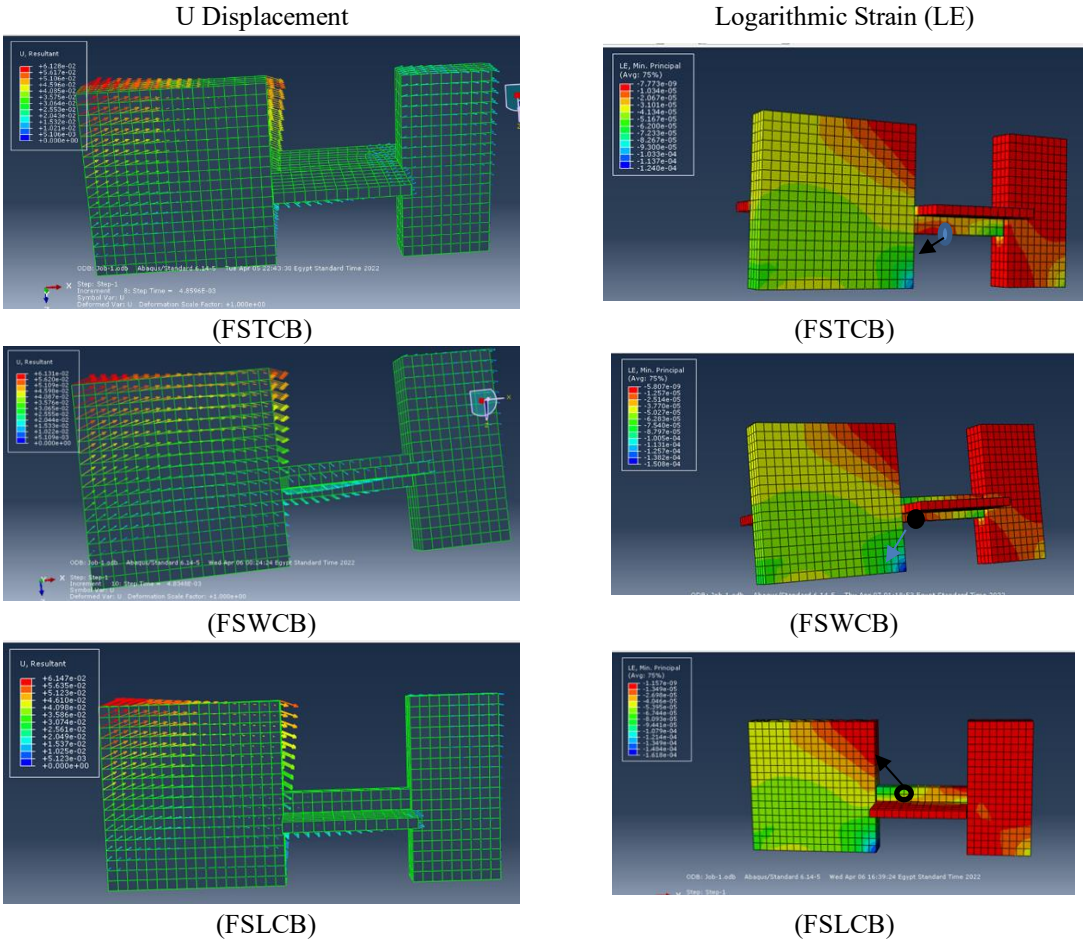

Fig. 26 Displacement and Logarithmic Strain (LE) for four stories

The simulation of CB models is only employed for four stories. In conclusion, all findings evidenced to be a good match with the previous analysis outcomes from ETABS and showing that:

Shear stress (τ) for (case 2: FSWCB) has values fewer than case1 (FSTCB)and case3 (FSLCB) by 8.8% and 6%, respectively. Figs. 25, and 27 describe the change in the stress values for the various models. So, the findings point to the effects of the SL on the CB.

Strain (Logarithmic Strain (LE)): There is a difference in strain behavior between different states. And, the (case 1: FSTCB) has a lowering in values by 20% and 26% in comparison to cases 2 (FSWCB) and case 3 (FSLCB). Also, Figs. 26, and 28 present the stress and displacement for all states.

The failure propagation in the CB arises at the position of maximum for both shear stress τ_{max} and principal stress, as designated in Fig. 25. The analysis shows that the best position of the CB for dropping the failure is case 2 (FSWCB) for four stories.

If the floor slab is explicitly modeled and a rigid diaphragm is assumed, the neutral axis for the CB cross section is at different positions (At top, within depth, at bottom). So, the neutral axis of CB is probably located at various slab level locations. This may significantly impact the stiffness

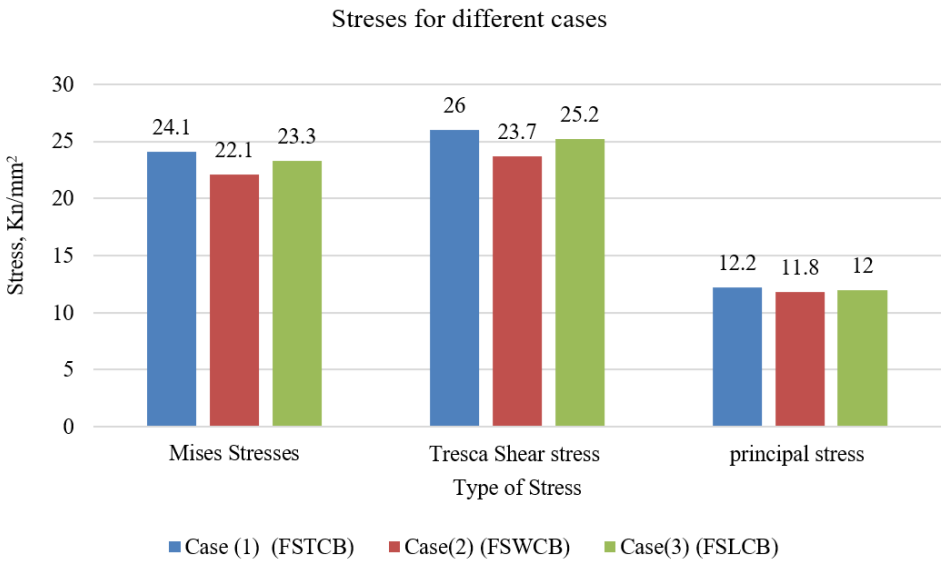

Fig. 27 Stress for different cases ((case 1: FSTCB), (case2:FSWCB), (case 3: FSLCB))

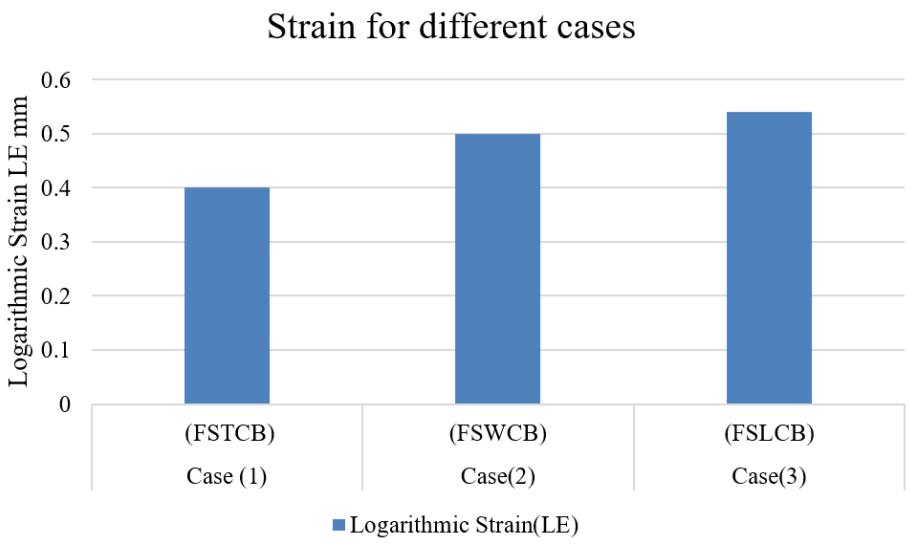

Fig. 28 Strain for different cases ((case 1: FSTCB), (case 2:FSWCB), (case 3: FSLCB))

and bending strength. Furthermore, the position of the rigidity connection of CB determines how the stress and strain distribution changes.

5. Conclusions

Numerical and experimental studies on the seismic behavior of coupled shear walls are insufficient, despite intensive testing of the enormous individual shear wall and the coupling beam.

As far as we are aware, no prior research has examined the effectiveness of the position of stiffness coupling between the SL and the CBs. And, despite the fact that the influence of CB position regarding the slab plate level is not taken into account in the design provisions, it has a gigantic impact on the seismic performance. Therefore, the effectiveness of the position of rigidity linkage between the SL and the CBs in the structure response for the seismic loading is examined through different cases (case1(FSTCB): FS at top of CB, case2(FSWCB): FS within panel depth of CB, case3(FSLCB): FS at the bottom of CB). On the other hand, this study gives a significant advantage because of the CB positions' contribution to reducing the response of structural buildings.

The behavior of the CB position is explored in 3-D models considering measured responses for the studied cases (four, eight, and twelve stories). Besides, the paper has concentrated on designating a 3-D FEM to comprehend the system's reactions in different states and hence getting suggestions for constructing a stable system. The main conclusions are that the position of the CB contributes to lower axial reactions, shear, moment, and lateral deformation. To abridge, the outcomes of analysis can be mentioned as proceeding:

In all models (four, eight, twelve stories): The finest position for rigidity connection amidst the CB and the SL for lowering lateral displacements is FS at top of the CB in relation to other cases (case2(FSWCB, case3(FSLCB). And, the finest position for rigidity linking among the CB and the SL for reducing axial force and shear force are recognized for FS within panel depth of CB compared to other cases ((case 1: FSTCB) and (case 3: FSLCB)). On the other hand, the perfect position for lowering moment is FS at bottom of CB in comparison to case 1: FSTCB, and case 2: FSWCB. Furthermore, case 1(FSTCB) has an impact on the lowering of displacement of the THS in relation to other cases. In addition, (case 3: FSLCB) reduces the acceleration of the THS in comparison to (case 1: FSTCB) for four stories. What's more, the positions of the CB have an extensive impact on the THS due to the location of stiffness connection. The outcomes of the stress and strains variant alternate depending on the locations of linking connections between the CB and the SL. In general, the simulation of the CB models which are utilized in ABAQUS software for four stories proves that all results are to be a good match with the previous outcomes from ETABS, and show that the shear stress for (case 2: FSWCB) has values fewer than other simulations ((case 1: FSTCB) and (case 3: FSLCB)). Future research should be devoted to analyzing the sensitivity of the slab thickness and reinforcement ratio with respect to different CB positions.

Authors' contributions

Yasser Abdelshafy Gamal: Conceptualization, methodology, Investigation, Writing-review editing of the original draft and submission; Idriss LK: Acquisition of data, analysis and interpretation and critical revision.

References

Abaqus, H.K. and Sorensen. (2001), ABAQUS Standard, User's Manual, Vol. 2, Version 6.2, Pawtucket, Hibbitt, Karlsson and Sorensen.

Abdel Raheem, S.E., Abdel Zaher, A.K. and Taha, A. (2018), "Finite element modeling assumptions impact

on seismic response demands of MRF-buildings", *Earthq. Eng. Eng. Vib.*, **17**(4), 821-834.
Álvarez, R., Restrepo, J.I., Panagiotou, M. and Godínez, S.E. (2020), "Analysis of reinforced concrete coupled structural walls via the Beam-Truss Model", *Eng. Struct.*, **220**, 111005. https://doi.org/10.1016/j.engstruct.2020.111005.
Aristizabal-Ocfaoa, J.D. (1987), "Seismic behavior of slender coupled wall systems", *J. Struct. Eng.*, **113**(10), 2221-2234. https://doi.org/10.1061/(ASCE)0733-9445(1987)113:10(2221).
Committee, A.C.I., American Concrete, I. (2020), Building Code Requirements for Structural Concrete (ACI 318-19), An ACI Standard.
Ding, R., Tao, M.X., Nie, X. and Mo, Y. (2018), "Analytical model for seismic simulation of reinforced concrete coupled shear walls", *Eng. Struct.*, **168**, 819-837. https://doi.org/10.1016/j.engstruct.2018.05.003.
Eljadei, A.A. (2012), *Performance based Design of Coupled Wall Structures,* University of Pittsburgh.
Engineers, A.S.O.C. (2000), *Minimum Design Loads for Buildings and other Structures*.
Fialko, S.Y. (2017), "Application of rigid links in structural design models", *Int. J. Comput. Civil Struct. Eng.*, **13**(3), 119-137. https://doi.org/10.22337/1524-5845-2017-13-3-119-137.
Galano, L. and Vignoli, A. (2000), "Seismic behavior of short coupling beams with different reinforcement layouts", *Struct. J.*, **97**(6), 876-885. https://doi.org/10.14359/518.
Harries, K.A., Gong, B. and Shahrooz, B.M. (2000), "Behavior and design of reinforced concrete, steel, and steel-concrete coupling beams", *Earthq. Spectra*, **16**(4), 775-799. https://doi.org/10.1193/1.1586139.
Idriss, L.K. and Gamal, Y.A.S. (2022), "The effect of a rigid connection between the slab and the coupled beam on the seismic performance of the coupling wall system", *J. Hunan Univ. Nat. Sci.*, **49**(1), 1. https://doi.org/10.55463/issn.1674-2974.49.1.31.
Kolozvari, K., Terzic, V., Miller, R. and Saldana, D. (2018), "Assessment of dynamic behavior and seismic performance of a high-rise rc coupled wall building", *Eng. Struct.*, **176**, 606-620. https://doi.org/10.1016/j.engstruct.2018.08.100.
Kumar, P., Kuldinow, D., Castillo, A., Gerakis, A. and Hara, K. (2021), "Nonlinear dynamics of coupled light and particle beam propagation", *Phys. Rev. A*, **103**(4), 043502. https://doi.org/10.1103/PhysRevA.103.043502.
Lim, E., Hwang, S.J., Cheng, C.H. and Lin, P.Y. (2016), "Cyclic tests of reinforced concrete coupling beam with intermediate span-depth ratio", *ACI Struct. J.*, **113**(3), 515.
Lu, X. and Chen, Y. (2005), "Modeling of coupled shear walls and its experimental verification", *J. Struct. Eng.*, **131**(1), 75-84. https://doi.org/10.1061/(ASCE)0733-9445(2005)131:1(75).
Ma, Y., Sun, B., Berman, J.W., Taoum, A. and Yang, Y. (2022), "Cyclic behavior of coupled steel plate shear walls with different beam-to-column connections", *J. Constr. Steel Res.*, **189**, 107084. https://doi.org/10.1016/j.jcsr.2021.107084.
Ma, Y., Yan, Z., Berman, J.W., Taoum, A. and Tian, W. (2022), "Seismic performance of coupled steel plate shear walls with different degrees of coupling", *J. Struct. Eng.*, **148**(9), 04022111. https://doi.org/10.1061/(asce)st.1943-541x.0003386.
Rezapour, M., Mirghaderi, S. and Rajabnejad, H. (2022), "Performance study of steel coupling beams in coupling shear-wall system", https://doi.org/10.21203/rs.3.rs-1767739/v1.
Santhakumar, A.R. (1974), "Ductility of coupled shear walls", Doctor of Philosophy, University of Canterbury, Civil Engineering.
Singh, V. and Sangle, K. (2022), "Analysis of vertically oriented coupled shear wall interconnected with coupling beams", *HighTech Innov. J.*, **3**(2), 230-242. https://doi.org/10.28991/hij-2022-03-02-010.
Tassios, T.P., Moretti, M. and Bezas, A. (1996), "On the behavior and ductility of reinforced concrete coupling beams of shear walls", *ACI Struct. J.*, **93**(6), 711-720.
Tian, J., Wang, Y., Jian, Z., Li, S. and Liu, Y. (2019), "Seismic performance and design method of PRC coupling beam-hybrid coupled shear wall system", *Earthq. Struct.*, **16**(1), 83-96. https://doi.org/10.12989/eas.2019.16.1.083.
Wang, T., Shang, Q., Wang, X., Li, J. and Kong, Z.A. (2018), "Experimental validation of RC shear wall structures with hybrid coupling beams", *Soil Dyn. Earthq. Eng.*, **111**, 14-30.

https://doi.org/10.1016/j.soildyn.2018.04.021.
Xuchuan, L., Xinzheng, L., Zhiwei, M., Lieping, Y., Yinquan, Y. and Lin, S. (2009), "Finite element analysis and engineering application of RC core-tube structures based on the multi-layer shell elements", *Chin. Civil Eng. J.*, **42**(3), 49-54.
Zuo, J.Q., Zhu, B.L., Guo, Y.L., Wen, C.B. and Tong, J.Z. (2022), "Experimental and numerical study of Steel Corrugated-Plate Coupling Beam connecting shear walls", *J. Build. Eng.*, 104662. https://doi.org/10.1016/j.jobe.2022.104662.

DC